Differentially Modulated Spectrally Efficient Frequency-Division Multiplexing

Seichiroh Osaki, *Student Member, IEEE*, Miyu Nakao, *Student Member, IEEE*,
Takumi Ishihara, *Student Member, IEEE*, and Shinya Sugiura, *Senior Member, IEEE*

***Abstract*—The present letter proposes a differentially modulated non-orthogonal spectrally efficient frequency-division multiplexing (D-SEFDM) architecture, which allows us to dispense with any pilot overhead needed for channel estimation at the receiver, while increasing the bandwidth efficiency in comparison to the orthogonal frequency-division multiplexing counterpart. While it is a challenging task to carry out differential-modulation-assisted non-coherent detection for multi-carrier transmissions in the presence of a severe inter-carrier interference (ICI), in the proposed scheme ICI elimination and symbol demodulation are implemented in a non-coherent manner, by exploiting the fact that ICI imposed by D-SEFDM is deterministically given, once we have a compression factor of non-orthogonal subcarriers. It is verified in our simulations that the proposed D-SEFDM exhibits a higher performance than the conventional coherent SEFDM scheme, especially for the scenarios of a high Doppler frequency.**

I. Introduction

THE classic differential modulation technique allows us to dispense with the pilot transmission and channel estimation (CE) [1], and hence the CE-error-induced performance degradation, which is typically imposed by its coherent counterpart, is avoided in differential non-coherent detection. Differential modulation was employed for orthogonal frequency-division multiplexing (OFDM) [2], by assuming that differentially modulated symbols in each subcarrier experience the non-dispersive frequency-flat channel. However, it is a challenging task to carry out such differential modulation and non-coherent detection in the frequency-selective channel, since equalization is inapplicable to non-coherent detection.

Introducing the concept of non-orthogonal resource allocation into several available domains, such as the time [3, 4], the frequency [5–8], and the power ones [9], have been investigated for improving the bandwidth efficiency, by allowing an increased processing complexity. More specifically, spectrally efficient frequency-division multiplexing (SEFDM) is a multicarrier transmission [5, 6], which relies on non-orthogonal subcarriers for the sake of improving a bandwidth efficiency, compared with the OFDM counterpart. Naturally, this SEFDM scheme's benefit is attained at the sacrifice of the additional demodulation complexity at the receiver, since inter-carrier interference (ICI) imposed has to be eliminated at the receiver [8, 10]. Note that as shown in [8], the SEFDM scheme's advantage over OFDM is attainable, especially in the low-rate transmission regime. Furthermore, multicarrier faster-than-Nyquist system was presented based on the exploitation of time- and frequency-domain non-orthogonal resource packing [11, 12].

Bearing the above background in mind, the novel contributions of this letter are as follows. We propose a differentially modulated SEFDM (D-SEFDM) scheme, where ICI introduced by non-orthogonal subcarriers of SEFDM is firstly canceled out at the receiver with the aid of the knowledge of subcarrier's compression factor. Then, differentially modulated symbols are demodulated in a non-coherent manner, i.e., without relying on any CE, similar to the conventional differential demodulation. Our simulation results clarify that the proposed D-SEFDM scheme exhibits the performance advantage over the conventional SEFDM scheme.

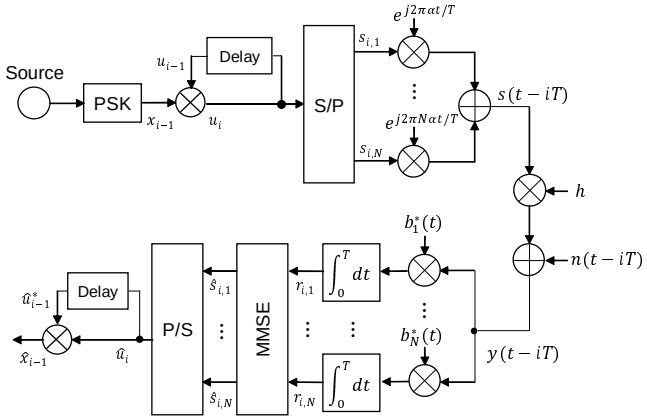

Fig. 1. Transceiver model of the proposed D-SEFDM scheme.

II. System Model of D-SEFDM

A. Transmitted Signal Model

Fig. 1 shows the system model of the proposed D-SEFDM transceiver. In this letter, we assume that the additive white-Gaussian noise (AWGN) and the frequency-flat Rayleigh fading channels. At the D-SEFDM transmitter, information bits are modulated with the aid of M-size phase-shift keying (PSK) constellation onto N subcarriers. The modulated PSK symbols are expressed by

$$\mathbf{x} = [x_1, x_2, \cdots, x_{BN-1}]^T \in \mathcal{C}^{BN-1}, \tag{1}$$

S. Osaki, M. Nakao, and T. Ishihara are with the Department of Computer and Information Sciences, Tokyo University of Agriculture and Technology, Koganei, Tokyo 184-8588, Japan.

S. Sugiura is with the Institute of Industrial Science, The University of Tokyo, Meguro-ku, Tokyo 153-8505, Japan (e-mail: sugiura@ieee.org). *(Corresponding author: Shinya Sugiura.)*

The present study was supported in part by the Japan Society for the Promotion of Science (JSPS) KAKENHI Grant Numbers 16KK0120, 17H03259, and 17K18871.

where $(BN-1)$ PSK symbols are generated in each frame that contains B blocks. Furthermore, N is the number of subcarriers.

Then, the PSK symbols $\mathbf{x}$ are differentially modulated, in order to generate differentially modulated PSK (DPSK) symbols $\mathbf{u} = [u_1, \cdots, u_{BN}]^T \in \mathcal{C}^{BN}$ as follows:

$$u_i = x_{i-1}u_{i-1} \quad (i = 2, \cdots, BN), \tag{2}$$

where the initial reference symbol is set to $u_1 = 1$. Furthermore, BN-length DPSK symbol vector $\mathbf{u}$ is rearranged to the $(N \times B)$-size matrix $\mathbf{S} = [\mathbf{s}_1, \cdots, \mathbf{s}_B] \in \mathcal{C}^{N\times B}$, where $\mathbf{s}_i = [s_{i,1}, \cdots, s_{i,N}]^T \in \mathcal{C}^N$. Here, we have the relationship of $u_{i+N(j-1)} = s_{j,i}$. This implies that differential encoding is carried out over an entire frame.

Then, the DPSK symbol $s_{i,j}$ is modulated onto the jth non-orthogonal subcarrier in the ith block, where the frequency-domain separation $\Delta f = \alpha/T$ between two adjacent subcarriers of the D-SEFDM scheme is lower than that of the OFDM counterpart. Furthermore, T is the block duration. Note that the no-compression case of $\alpha = 1$ corresponds to the classic OFDM scenario.

The transmitted signals of D-SEFDM in the ith block is given by

$$s(t - iT) = \frac{1}{\sqrt{T}} \sum_{k=1}^{N} s_{i,k} \exp(j2\pi k\alpha t/T). \tag{3}$$

Moreover, since the bandwidth consumed by the D-SEFDM scheme is given by [13]

$$\frac{(N-1)\alpha}{T} + \frac{2}{T} \text{ [Hz]}, \tag{4}$$

the bandwidth efficiency R is formulated by

$$R = \frac{(BN-1)\log_2 M}{B[(N-1)\alpha + 2]} \text{ [bps/Hz]}. \tag{5}$$

B. Received Signal Model

Let us assume that the SEFDM frame is transmitted to the receiver over the quasi-static frequency-flat Rayleigh fading channel, and then the received signals in the ith block $y(t-iT)$ are represented by

$$y(t - iT) = hs(t - iT) + n(t - iT), \tag{6}$$

where $n(t - iT)$ is the AWGN components, which are represented by the random variables, obeying the complex-valued Gaussian distribution of $\mathcal{CN}(0, N_0)$ with a zero mean and a noise variance of N_0. Also, h is a channel coefficient, which obeys the distribution of $\mathcal{CN}(0, 1)$. Moreover, the channel coefficient h is assumed to remain constant over the two successive block intervals, while the exact knowledge of the compression factor α and the noise variance N_0 is acquired at the receiver in advance.

At the receiver, the received signals are initially processed by N correlators that extract a set of sufficient statistics, in order to eliminate the effects of colored noises. The output of the ith receiver correlator in the ith frame is expressed as

$$r_{i,j} = \int_0^T y(t - iT)b_j^*(t)dt \quad (j = 1, \cdots, N), \tag{7}$$

where $b_j(t)$ is the jth component of an orthonormal basis generated according to the Gram-Schmidt orthonormalization [5]. Hence, we arrive at

$$\mathbf{r}_i = [r_{i,1}, \cdots, r_{i,N}]^T \in \mathcal{C}^N, \tag{8}$$

$$= h\mathbf{M}\mathbf{s}_i + \mathbf{n}_i, \tag{9}$$

where the matrix $\mathbf{M} \in \mathcal{C}^{N\times N}$ represents the correlation coefficients. The pth-row and qth-column element of $\mathbf{M}$ is given by

$$m_{p,q} = \frac{1}{\sqrt{T}} \int_0^T \exp(j2\pi q\alpha t/T)b_p^*(t)dt. \tag{10}$$

Also, $\mathbf{n}_i = [n_{i,1}, \cdots, n_{i,N}]^T \in \mathcal{C}^N$ is the associated noise component, which is given by

$$n_{i,k} = \frac{1}{\sqrt{T}} \int_0^T n(t - iT)b_k^*(t)dt. \tag{11}$$

Note that the matrix $\mathbf{M}$ is available at the receiver, since it is uniquely determined by the compression factor α.

Then, based on the minimum mean-square error (MMSE) criterion [14], we arrive at

$$\hat{\mathbf{s}}_i = [\hat{s}_{i,1}, \cdots, \hat{s}_{i,N}]^T \in \mathcal{C}^N \tag{12}$$

$$= \mathbf{W}\mathbf{r}_i \tag{13}$$

$$= h\mathbf{W}\mathbf{M}\mathbf{s}_i + \mathbf{W}\mathbf{n}_i, \tag{14}$$

where the MMSE weights $\mathbf{W} \in \mathcal{C}^{N\times N}$ are given by

$$\mathbf{W} = \mathbf{M}^H(\mathbf{M}\mathbf{M}^H + N_0\mathbf{I}_N)^{-1}. \tag{15}$$

Note that $\mathbf{M}^H$ denotes the hermitian of matrix $\mathbf{M}$ and $\mathbf{I}_N$ is the identity matrix with the size of N. Moreover, $\hat{\mathbf{s}}_i$ are rearranged to $\hat{\mathbf{u}} = [\hat{u}_1, \cdots, \hat{u}_{BN}]^T \in \mathcal{C}^{BN}$, according to $\hat{u}_{i+N(j-1)} = \hat{s}_{j,i}$.

Finally, similar to [15, 16], the PSK symbols $\hat{\mathbf{x}} = [\hat{x}_1, \cdots, \hat{x}_{BN-1}]^T \in \mathcal{C}^{BN-1}$ are estimated from the equalized D-SEFDM symbols $\hat{\mathbf{u}}$ as follows:

$$\hat{x}_{i-1} = \arg\min_{x_{i-1}} \|x_{i-1} - \hat{u}_i\hat{u}_{i-1}^*\| \quad (i = 2, \cdots, BN). \tag{16}$$

Hence, the channel coefficient h does not have to be estimated at our D-SEFDM receiver.

Note that the complexity orders of (13), (15), and (16), which are evaluated in terms of the number of real-valued multiplications and additions, are given by $\mathcal{O}(N^2)$, $\mathcal{O}(N^3)$, and $\mathcal{O}(N)$, respectively. However, by relying on the fact that the matrix M is known in advance of transmissions, the calculations of (15) can be carried out offline, over the potential range of the noise variance N_0. Hence, the total complexity order per block of the presented successive detection algorithm is as low as $\mathcal{O}(N^2)$, which is tractable even in a mobile handset.

C. Analytical Bit-Error Ratio

Here, we provide the bit-error ratio (BER) of the proposed D-SEFDM scheme. From (14), the components of the desired D-SEFDM symbols, the ICI, and the AWGNs are represented, respectively, by $\mathbf{s}_d = h\mathbf{\Gamma}_d\mathbf{s}$, $\mathbf{s}_I = h\mathbf{\Gamma}_I\mathbf{s}$, and $\mathbf{s}_n = \mathbf{W}\mathbf{n}$. Here, we have $\mathbf{\Gamma}_d = \text{diag}\{\mathbf{WM}\}$ and $\mathbf{\Gamma}_I = \mathbf{WM} - \mathbf{\Gamma}_d$. Then, the

average power of the desired D-SEFDM symbols, the ICI and the AWGN components are given by

$$P_d = \mathrm{tr}\{\mathrm{E}[\mathbf{s}_d\mathbf{s}_d^H]\} = \mathrm{tr}\{\mathrm{E}[hh^*\mathbf{\Gamma}_d\mathbf{s}\mathbf{s}^H\mathbf{\Gamma}_d^H]\} = \mathrm{tr}\{\mathbf{\Gamma}_d\mathbf{\Gamma}_d^H\}. \quad (17)$$

$$P_I = \mathrm{tr}\{\mathrm{E}[\mathbf{s}_I\mathbf{s}_I^H]\} = \mathrm{tr}\{\mathrm{E}[hh^*\mathbf{\Gamma}_I\mathbf{s}\mathbf{s}^H\mathbf{\Gamma}_I^H]\} = \mathrm{tr}\{\mathbf{\Gamma}_I\mathbf{\Gamma}_I^H\} \quad (18)$$

$$P_n = \mathrm{tr}\{\mathrm{E}[\mathbf{s}_n\mathbf{s}_n^H]\} = \mathrm{tr}\{\mathrm{E}[\mathbf{W}\mathbf{n}\mathbf{n}^H\mathbf{W}^H]\} = \mathrm{tr}\{\mathbf{W}\mathbf{W}^H\}N_0. \quad (19)$$

Note that (17) and (18) come from the relationships of $\mathrm{E}[hh^*] = 1$ and $\mathrm{E}[\mathbf{s}\mathbf{s}^H] = \mathbf{I}_N$. Also, (19) comes from the relationship of $\mathrm{E}[\mathbf{n}\mathbf{n}^H] = N_0\mathbf{I}_N$. From (17)–(19), the average SINR value of the D-SEFDM symbols is given by

$$\mathrm{SINR}_b = \frac{1}{\log_2 M} \times \frac{P_d}{P_I + P_n}. \quad (20)$$

Since the analytical average BER of differential BPSK is formulated by [17]

$$P(E) = \frac{1}{2(1+\gamma_b)}, \quad (21)$$

the analytical BER of DBPSK-modulated D-SEFDM scheme over a frequency-flat Rayleigh fading channel is derived by substituting (20) into the γ_b of (21). Similarly, the analytical average BERs of differential QPSK, 8PSK, and 16PSK [17] are readily applicable to our analytical framework.

III. Performance Investigations

Our performance results are provided for characterizing the achievable performance of the proposed D-SEFDM scheme. The number of subcarriers and that of blocks per frame were given by $N = 4$ and $B = 256$, respectively. Furthermore, we assumed the transmissions of sinc pulses for the modulated symbols of each subcarrier. Hence, $b_j(t)$ is represented by the window function. Unless otherwise noted, these parameters were used throughout this section. The conventional coherent SEFDM and OFDM were considered to be benchmark schemes. We evaluated the proposed D-SEFDM scheme for both the quasi-static and time-varying frequency-flat Rayleigh fading channels.[1]

Firstly, in Fig. 2 we show the BER performance of the proposed D-SEFDM scheme in the quasi-static frequency-flat Rayleigh fading channel. Here, we plotted both the numerical and analytical curves. Fig. 2(a) shows the BPSK-modulated D-SEFDM scheme with the compression factor of $\alpha = 0.7, 0.8,$ and 0.9, which corresponded to the bandwidth efficiencies of 0.85, 0.91 and 0.98 [bps/Hz]. Fig. 2(b) shows the D-SEFDM scheme, employing BPSK, QPSK, 8PSK, and 16PSK, while maintaining $\alpha = 0.8$. As shown in Fig. 2(a), the proposed D-SEFDM with $\alpha = 0.9$ exhibited a similar performance to the conventional DBPSK-modulated OFDM ($\alpha = 1.0$), while attaining a 6% higher bandwidth efficiency than that of the

[1]In this letter, we assumed the frequency-flat fading channel, similar to the conventional SEFDM studies. However, incorporation of blind CE of the dispersive channel coefficients may be useful for successful operation of non-coherent detection of the proposed D-SEFDM scheme in the frequency-selective fading channel, which is left for our future study.

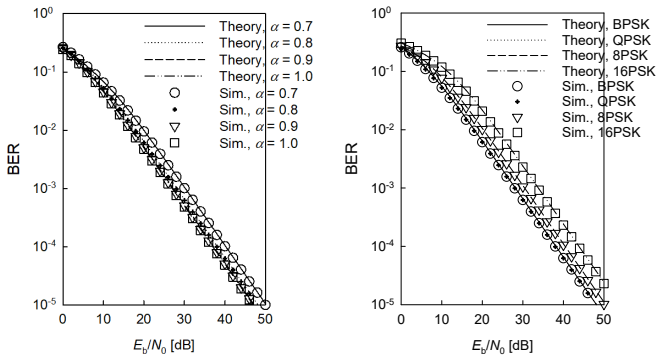

(a) BPSK, $\alpha = 1.0$, 0.9, 0.8, and 0.7 (b) $\alpha = 0.8$, BPSK, QPSK, 8PSK, and 16PSK

Fig. 2. The achievable BER performance of the D-SEFDM scheme, where both the numerical and analytical curves were plotted.

OFDM counterpart. Note that the analytical and numerical curves well matched, hence validating the system model of the proposed D-SEFDM scheme. Furthermore, the D-SEFDM scheme with $\alpha = 0.7$ achieved a 23% higher bandwidth efficiency than OFDM, while suffering from a 3-dB performance penalty. Observe in Fig. 2(b) that regardless of the modulation order, the analytical curves were coincided with the numerical counterparts.

Next, Fig. 3 compares the BERs of the proposed D-SEFDM scheme and the conventional coherent SEFDM scheme, each employing the MMSE equalizer at the receiver, where BPSK and QPSK were considered in Figs. 3(a) and 3(b), respectively. It is assumed that in the conventional coherent SEFDM, the accurate CSI was used at the receiver, and that the rate reduction due to the pilot overhead was ignored. As seen in Fig. 3, in each α scenario, a 3-dB performance loss was observed in the D-SEFDM scheme over the conventional coherent SEFDM scheme. This loss was due to the well-known noise-doubling effects, which are caused by differential demodulation [1]. Hence, the fundamental performance merits of the D-SEFDM scheme over the conventional OFDM with differential encoding, is similar to those of the SEFDM scheme over coherent OFDM, which was shown in [5–12].

Moreover, we considered the scenarios of the time-varying frequency-flat Rayleigh fading channels. Fig. 4 shows the achievable BERs of the BPSK-modulated D-SEFDM and the conventional BPSK-modulated coherent SEFDM, where α was fixed to 0.8. Note that the received signals of (6) are changed to $y(t-iT) = h(t)s(t-iT)+n(t-iT)$, where $h(t)$ is the fading coefficients of the time-varying channel, which obeys the relationship of $E[h(t)h^*(t+\tau)] = J_0(2\pi F_d T\tau)$. Here, F_dT represents the normalized Doppler frequency, and J_0 is the zero-order Bessel function of the first kind. For the coherent scheme, we assumed that the accurate CSI was updated at the beginning of each frame. Observe in Fig. 4 that the coherent SEFDM suffered from an error floor in the scenarios of $F_dT = 1.0 \times 10^{-5}$ and 1.0×10^{-6}, while the D-SEFDM scheme maintained the error-floor-free performance, which is comparable to the quasi-static scenario of Fig. 3.

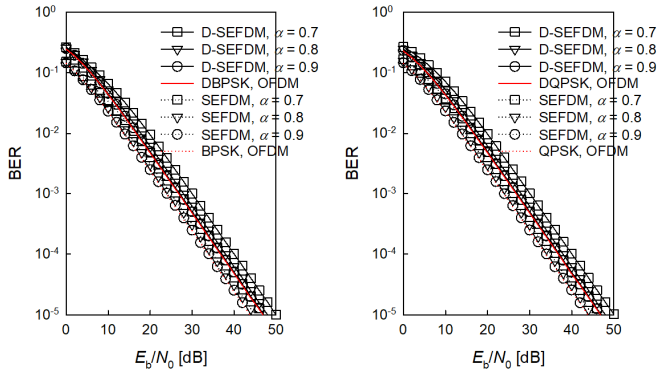

(a) BPSK (b) QPSK

Fig. 3. The achievable BERs of the proposed D-SEFDM and the conventional coherent SEFDM, the bandwidth compression factor was set to $\alpha = 1.0, 0.9, 0.8$, and 0.7: (a) BPSK, (b) QPSK.

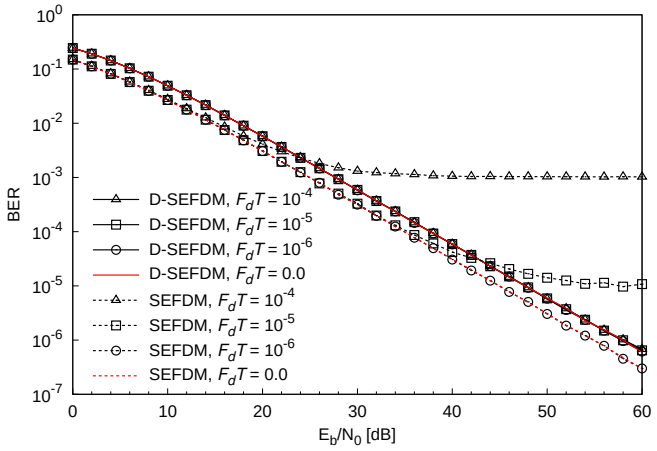

Fig. 4. The achievable BERs of the proposed D-SEFDM and the conventional coherent SEFDM in the time-varying frequency-flat Rayleigh fading channels, both employing the BPSK and the number of blocks of $B = 256$. Here, the compression factor was fixed to $\alpha = 0.8$. The normalized Doppler frequencies were set to $F_dT = 1.0 \times 10^{-6}, 1.0 \times 10^{-5}$, and 1.0×10^{-4}.

Next, Fig. 5 illustrates the effects of the compression factor α on the BER performance. Here, the compression factor was varied from $\alpha = 0.3$ to 1.0 and $\mathrm{E}_b/\mathrm{N}_0$ was maintained to 40 dB. Observe in Fig. 5 that the D-SEFDM scheme remained unchanged, regardless of F_dT, even if α was small. By contrast, the BER of the coherent SEFDM deteriorated, upon increasing the normalized Doppler frequency. More specifically, the performance of the coherent SEFDM scheme with $F_dT = 1.0 \times 10^{-4}$ explicitly outperformed by the proposed D-SEFDM scheme for $\alpha \geq 0.5$.

Fig. 6 shows the BER performance of the proposed D-SEFDM scheme and the conventional SEFDM schemes, both employing BPSK modulation, which ere recorded at the $\mathrm{E}_b/\mathrm{N}_0 = 40$ dB, where the number of blocks was varied from $B = 64$ to 2048, and the compression factor was maintained to $\alpha = 0.8$. It was found from Fig. 6 that the BER performance of the D-SEFDM scheme remained almost unchanged, regardless of the number of blocks B and the

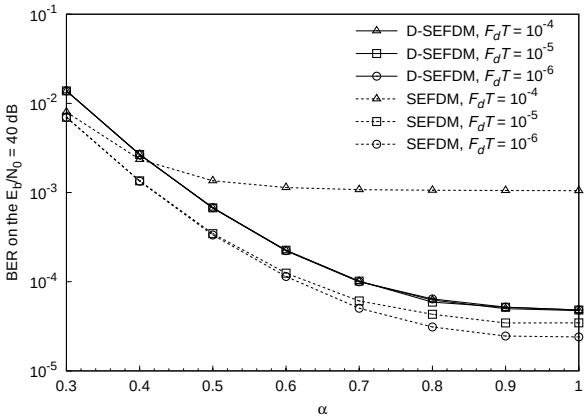

Fig. 5. The effects of the compression factor α on the achievable BERs of the proposed D-SEFDM and the conventional SEFDM schemes, both employing BPSK modulation, which were recorded at the $\mathrm{E}_b/\mathrm{N}_0 = 40$ dB in the time-varying frequency-flat Rayleigh fading channels. The compression factor was varied from $\alpha = 0.3$ to 1.0.

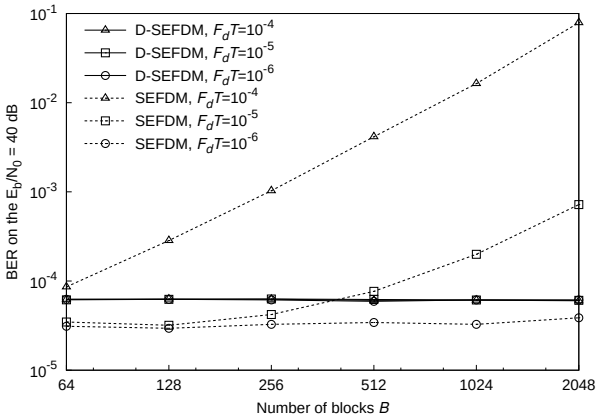

Fig. 6. The BER performance of the proposed D-SEFDM and the conventional SEFDM schemes, both employing BPSK modulation, which were recorded at the $\mathrm{E}_b/\mathrm{N}_0$ of 40 dB in the time-varying frequency-flat Rayleigh fading channel, where the number of blocks was varied from $B = 64$ to 2048. Here the compression factor was set to $\alpha = 0.8$.

normalized Doppler frequencies F_dT. By contrast, the BER performance of the coherent SEFDM scheme was largely affected, and more specifically, its BER performance was deteriorated, upon increasing the number of blocks.

Essentially, the PAPRs of the D-SEFDM and the SEFDM schemes are identical, since the main difference between both the transmitters are constituted by differential encoding of (16), employed by D-SEFDM. Note that in our extensive numerical studies, the PAPRs of the SEFDM, D-SEFDM, and OFDM schemes were found to be comparable.

IV. Conclusions

The present letter proposed the novel D-SEFDM scheme, which is capable of CE-free non-coherent detection, despite the effects of ICI. This is enabled by exploiting the fact that ICI is accurately attained at the receiver in a deterministic manner. Furthermore, it was shown that our proposed D-SEFDM outperformed the conventional SEFDM in the scenarios of a high Doppler-frequency.

REFERENCES

[1] L. Hanzo, S. Ng, W. T. Webb, and T. Keller, *Quadrature amplitude modulation: From basics to adaptive trellis-coded, turbo-equalised and space-time coded OFDM, CDMA and MC-CDMA systems*. John Wiley and IEEE Press, 2004.

[2] L. Wang, L. Li, C. Xu, D. Liang, S. X. Ng, and L. Hanzo, "Multiple-symbol joint signal processing for differentially encoded single- and multi-carrier communications: Principles, designs and applications," *IEEE Communications Surveys and Tutorials*, vol. 16, no. 2, pp. 689–712, 2014.

[3] J. Anderson, F. Rusek, and V. Owall, "Faster-than-Nyquist signaling," *Proceedings of the IEEE*, vol. 101, no. 8, pp. 1817–1830, Aug. 2013.

[4] S. Sugiura, T. Ishihara, and M. Nakao, "State-of-the-art design of index modulation in the space, time, and frequency domains: Benefits and fundamental limitations," *IEEE Access*, vol. 5, pp. 21 774–21 790, 2017.

[5] M. Rodrigues and I. Darwazeh, "A spectrally efficient frequency division multiplexing based communications system," in *Proc. 8th International OFDM Workshop*, Hamburg, Germany, Sept. 2003, pp. 48–49.

[6] P. N. Whatmough, M. R. Perrett, S. Isam, and I. Darwazeh, "VLSI architecture for a reconfigurable spectrally efficient FDM baseband transmitter," *IEEE Transactions on Circuits and Systems I: Regular Papers*, vol. 59, no. 5, pp. 1107–1118, May 2012.

[7] I. Darwazeh, H. Ghannam, and T. Xu, "The first 15 years of SEFDM: A brief survey," in *11th International Symposium on Communication Systems, Networks & Digital Signal Processing*. IEEE, 2018, pp. 1–7.

[8] M. Nakao and S. Sugiura, "Spectrally efficient frequency division multiplexing with index-modulated non-orthogonal subcarriers," *IEEE Wireless Communications Letters*, vol. 8, no. 1, pp. 233–236, Feb. 2019.

[9] L. Dai, B. Wang, Y. Yuan, S. Han, I. Chih-Lin, and Z. Wang, "Non-orthogonal multiple access for 5G: solutions, challenges, opportunities, and future research trends," *IEEE Communications Magazine*, vol. 53, no. 9, pp. 74–81, Sept. 2015.

[10] K. Park, H. Kim, A. Lee, D. Kang, and W. Oh, "Iterative frequency-domain inter-carrier interference cancellation for coded SEFDM," *Electronics Letters*, vol. 53, no. 19, pp. 1333–1335, 2017.

[11] A. Barbieri, D. Fertonani, and G. Colavolpe, "Time-frequency packing for linear modulations: spectral efficiency and practical detection schemes," *IEEE Transactions on Communications*, vol. 57, no. 10, pp. 2951–2959, Oct. 2009.

[12] D. Dasalukunte, F. Rusek, and V. Owall, "Multicarrier faster-than-Nyquist transceivers: Hardware architecture and performance analysis," *IEEE Transactions on Circuits and Systems I: Regular Papers*, vol. 58, no. 4, pp. 827–838, Apr. 2011.

[13] I. D. Kanaras, "Spectrally efficient multicarrier communication systems: signal detection, mathematical modelling and optimisation," Ph.D. dissertation, University College London, 2010.

[14] I. Kanaras, A. Chorti, M. R. D. Rodrigues, and I. Darwazeh, "A combined MMSE-ML detection for a spectrally efficient non orthogonal FDM signal," in *5th International Conference on Broadband Communications, Networks and Systems*, Sept. 2008, pp. 421–425.

[15] T. Ishihara and S. Sugiura, "Differential faster-than-Nyquist signaling," *IEEE Access*, vol. 6, pp. 4199–4206, 2018.

[16] C. Sagayama, T. Ishihara, and S. Sugiura, "Performance analysis and constellation optimization of star-QAM-aided differential faster-than-Nyquist signaling," *IEEE Signal Processing Letters*, vol. 26, no. 1, pp. 144–148, Jan. 2019.

[17] M. K. Simon and M. S. Alouini, *Digital communication over fading channels*. Wiley-IEEE Press, 2005.